1. Paweł REGULSKI, 2. Waldemar REBIZANT, 3. Matthias KEREIT

ORCID: 1. 0000-0002-6076-2627; 2. 0000-0002-7508-366X

Measurement of line propagation velocity from line closing test in hybrid line configurations

Pomiar prędkości propagacji fali na podstawie testu załączenia linii w przypadku konfiguracji mieszanych linii

Abstract. The paper presents analysis of line propagation velocity measurement from a line closing test with the focus on hybrid line configurations. It describes traveling wave extraction methodology and provides methods of calculation of the line propagation velocity from the timing of specific travelling wave reflections for selected hybrid configurations. Analysis of the impact of line propagation error on the accuracy of fault location is provided for single-ended and double-ended approaches.

Streszczenie. Artykuł przedstawia analizę pomiaru prędkości propagacji fali na podstawie testu załączenia linii skupiającą się na mieszanych konfiguracjach linii. Opisany został sposób ekstrakcji informacji o falach wędrujących oraz metody obliczeń prędkości propagacji fali opierające się o czas poszczególnych odbić dla wybranych konfiguracji linii mieszanych. Zawarta została również analiza wpływu błędu prędkości propagacji na dokładność lokalizacji miejsca zwarcia dla algorytmów wykorzystujących pomiary tylko z jednego końca linii oraz z obu końców.

Keywords: travelling wave, fault location, filtering, wave propagation velocity
Słowa kluczowe: fala wędrująca, lokalizacja zwarcia, filtracja, prędkość propagacji fali

Introduction

A constant drive to reduce operation times of transmission line protection schemes and advancement of available technology allow for application of novel fault detection and location approaches. One such approach gaining attention in recent years is the utilization of travelling waves (TWs) [1-13]. This includes single-ended approaches [8-11], which utilize measurements from one end only, as well as double-ended approaches [1-7], which require information from both line ends. Multi-measuring points along a line are also proposed in [12]. Most common approach is based on the timing of specific TWs, which allows extraction of the information about the location of the source of disturbance. These solutions rely on the knowledge of line propagation velocity for TW-based fault location. However, accurate value of this quantity is rarely known to the system operator. One practical approach to obtaining line propagation velocity is performing a line closing test, in which line energized at one end becomes energized at the other end. This is provoking TWs to travel from a known location (one line end) and reflect from discontinuities (line ends, line-cable junctions). At the same time high resolution measurements are being captured. This data is then analysed, TWs are identified and time-stamped and line propagation times for different sections can be calculated. This is especially important for hybrid line configurations, as different sections will have different propagation velocities, all of which will impact the overall accuracy of fault location.

This paper provides analysis of different ways of calculating the line propagation velocity, with the focus on hybrid line configurations. This includes a case with a very short cable section to assess the applicability of such approach. Next, the influence of line propagation velocity on fault location is tested using both single-ended approach, as well as double-ended approach. The necessary simulations are performed in PSCAD, and the analysis is conducted in Matlab.

Travelling wave extraction

The processing starts by applying the Clarke transformation [1]. This is done in order to eliminate the effect of mutual coupling, similarly to symmetrical components. It should be noted that this transformation is applied directly to 3-phase instantaneous values according to the transformation matrix (1). Next, the first aerial mode (α) is used for traveling wave extraction.

(1)
$$\begin{bmatrix} 0 \\ \alpha \\ \beta \end{bmatrix} = \frac{2}{3} \begin{bmatrix} \frac{1}{2} & \frac{1}{2} & \frac{1}{2} \\ 1 & -\frac{1}{2} & -\frac{1}{2} \\ 0 & \frac{\sqrt{3}}{2} & -\frac{\sqrt{3}}{2} \end{bmatrix} \begin{bmatrix} a \\ b \\ c \end{bmatrix}$$

Wavelet transform is one of the most popular ways of extracting details of signals, especially useful for travelling wave analysis, since it also offers the location in time of specific frequencies. In practice this is equivalent to applying a finite impulse response (FIR) filter of specific coefficients. One popular family of wavelets is the Daubechies family [14]. One example is the db2 wavelet, which can successfully extract the high-frequency content of a signal. As an alternative, this paper proposes a different approach, namely a first order Walsh filter [15], impulse response of which is depicted in fig. 1.
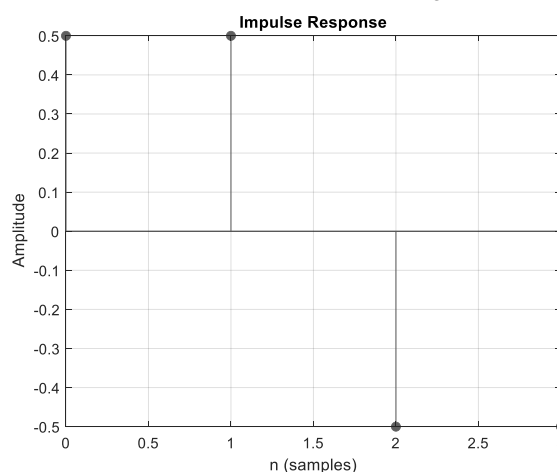

Fig.1. Impulse response of first order Walsh filter

Frequency response of the db2 wavelet equivalent and the proposed Walsh filter are shown in fig. 2. It can be observed that the wavelet acts as a high-pass filter with gain greater than 1 in the pass band, which means that a high-frequency noise might be amplified. On the other hand,

the Walsh filter attenuates the highest frequencies. In time domain the proposed approach more accurately represents the amplitude of a step signal.
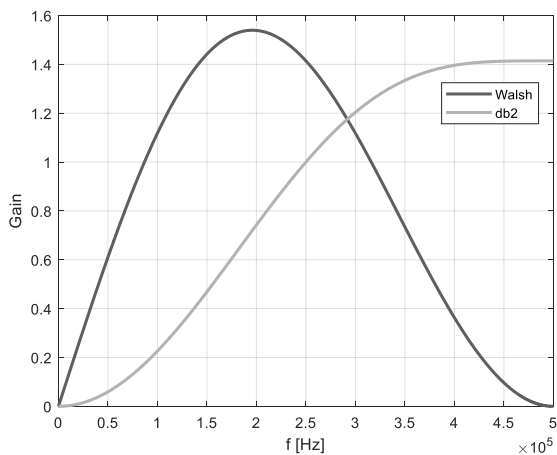

Fig.2. Frequency response of a db2 wavelet and first order Walsh filter

All of the calculations are conducted assuming 1 MHz sampling frequency of measurements.

Test systems

The measurements necessary for performing the analysis were obtained from computer simulations conducted in PSCAD. Two different configurations were modelled: line-cable configuration and line-cable-line configuration (fig. 3). Additionally, the first configuration has two versions – one with 10 km cable section and one with 0.5 km cable section.
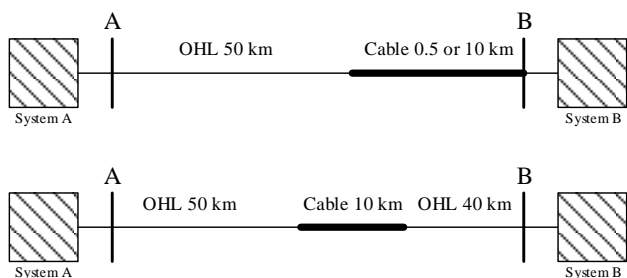

Fig.3. The single-line diagrams of different line configurations considered in this study.

The voltage of the network is 110 kV. System A has a short-circuit capacity of 2 GVA and System B of 1 GVA. Overhead line parameters are given in table 1. Cable cross-section is shown in fig. 4 and the corresponding parameters are given in table 2. The three cable conductors are arranged flat formation one meter underground 20 cm apart (measured from the middle of each conductor).

Table 1. Overhead line parameters

Cond.	Inner radius [m]	Outer radius [m]	DC resistance [Ω/km]	x [m]	y [m]	Sag [m]
1	0.00405	0.01085	0.124	-2.8	13	7
2	0.00405	0.01085	0.124	3.6	13	7
3	0.00405	0.01085	0.124	2.8	16.6	7

The maximum propagation velocities for the line and cable sections are 299.6119 km/ms and 197.5284 km/ms, respectively. It should be noted that due to wave dispersion, the measured line propagation velocities are expected to be slightly lower. This effect is the reason why the shape of a wave is somewhat different as it travels along a conductor.

The wave becomes stretched, and the timing of the peak value becomes slightly delayed, hence the lowered obtained propagation velocity. Propagation velocity calculated from measurements captures the dispersion effect and for this reason the fault location algorithms do not require compensation [1].
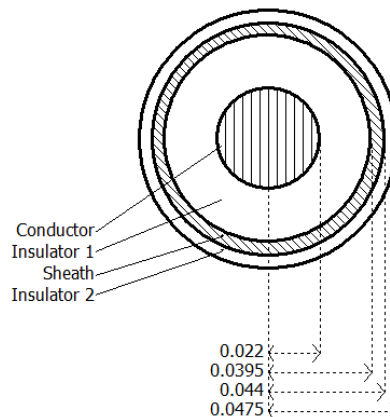

Fig.4. The single-line diagrams of different line configurations considered in this study.

Table 2. Cable parameters

Parameter	Value
Conductor resistivity [Ω*m]	1.68e-8
Insulator 1 relative permittivity	2.3
Sheath resistivity [Ω*m]	2.2e-7
Insulator 2 relative permittivity	2.3

Line-cable configuration

It is assumed that the circuit breaker (CB) closing test is performed at the A side of the line. The expected pattern of TW reflections and their corresponding arrival times at either line end are depicted in fig. 5.
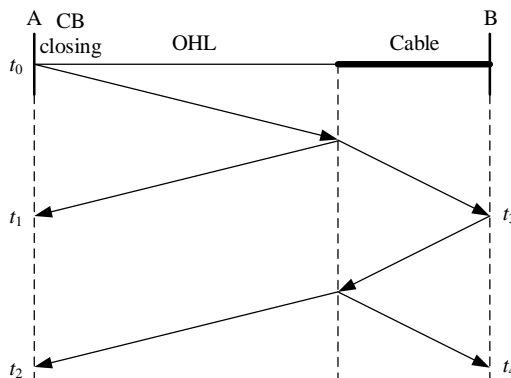

Fig.5. Expected pattern of TW reflections for line-cable configuration

The propagation velocities of each section can be calculated in several ways, depending on the source of measurements. Assuming the availability of measurements only from side A, the propagation velocities can be calculated as follows:

$$（2）\quad v_{line} = \frac{2l_{line}}{t_1 - t_0}$$

$$（3）\quad v_{cable} = \frac{2l_{cable}}{t_2 - t_1}$$

where: l_{line} – length of overhead line section, km, l_{cable} – length of cable section, km.

Cable section propagation velocity can also be calculated based on measurements obtained from side B (4). It has been observed that it is more difficult to observe reflections allowing for calculation of line section propagation velocity at side B.

$$(4) \qquad v_{cable} = \frac{2l_{cable}}{t_4 - t_3}$$

Fig. 6 shows the extracted TWs from 3-phase current measurements at both ends of the line. Observing the amplitude of reflections it can be concluded that the cable section shows much stronger attenuation, which is as expected. Exactly for this reason it is more difficult to capture TWs at the B side of the line.
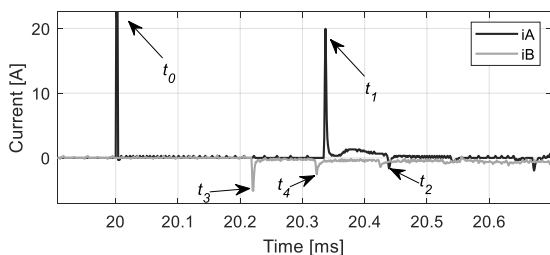

Fig.6. Extracted TWs for line-cable configuration

Table 3 presents the calculated propagation velocities using all three formulas. It can be observed that the values for both sections are very close to the expected maximum propagation velocities mentioned previously. The difference is well below 1% in both cases. Also, calculation of cable section propagation velocity gives the same result with (3) and (4).

Table 3. Calculation of propagation velocities for line-cable configuration

Parameter	Value
v_{line} (2)	298.507 km/ms
v_{cable} (3)	196.078 km/ms
v_{cable} (4)	196.078 km/ms

The same analysis has been repeated for this configuration, but with the cable section reduced to 0.5 km. This case is expected to produce a sequence of very fast reflections due to short distance between junctions.

Fig. 7 shows the captured TWs at both ends of the line and fig. 8 shows a close up view of the fast TW reflections captured at side B.
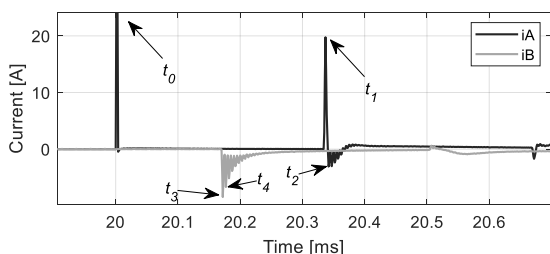

Fig.7. Extracted TWs for line-cable configuration (short cable section case)

In the case of a short cable section it can be observed that the sampling frequency of 1 MHz starts to become a limiting factor, as the resolution becomes insufficient to capture the TW details. The calculated propagation velocities are presented in table 4. The propagation velocity of the line section has the same value as in the previous test, but the short cable section results in a larger error. It

should be noted that given such a short cable section and the assumed sampling frequency, an error of one sample produces a very high error of the calculated propagation velocity. Running a series of simulations and increasing the cable section by 200 m each time it has been found, that the minimum recommended cable length is 2,5 km. Below this value the method may yield unacceptable propagation velocity error. Otherwise, the sampling frequency should be increased accordingly. In the case of 0.5 km cable section this should be at least 5 MHz
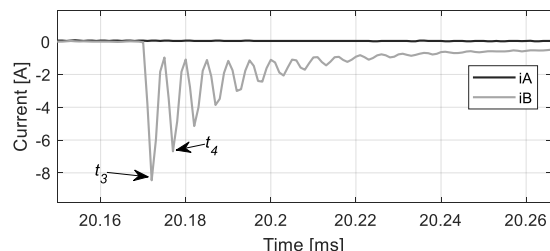

Fig.8. Extracted TWs for line-cable configuration (short cable section) – close up view of side B reflections

Table 4. Calculation of propagation velocities for line-cable configuration (short cable section case)

Parameter	Value
v_{line} (2)	298.507 km/ms
v_{cable} (3)	200.000 km/ms
v_{cable} (4)	200.000 km/ms

Line-cable-line configuration

The second hybrid line configuration consists of three sections, one of which is a cable. The line closing test is also initiated at side A. The expected pattern of TW reflections and their corresponding arrival times at either line end are depicted in fig. 9.
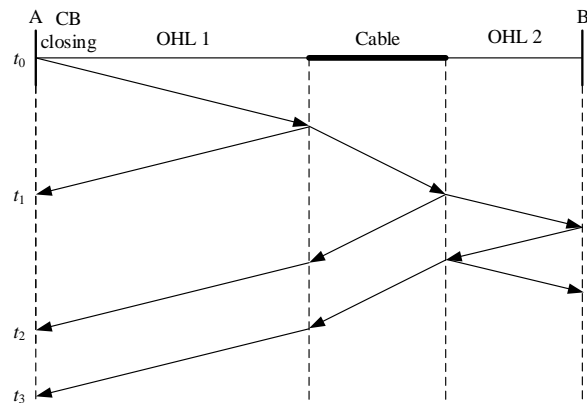

Fig.9. Expected pattern of TW reflections for line-cable-line configuration

The propagation velocities of each section can be also calculated in several ways, depending on the source of measurements. Assuming the availability of measurements only from side A, the propagation velocity of the cable section is calculated by (3) and the velocities of line sections can be calculated as follows:

$$(5) \qquad v_{line1} = \frac{2l_{line1}}{t_1 - t_0}$$

$$(6) \qquad v_{line2} = \frac{2l_{line2}}{t_3 - t_2}$$

where: l_{line1} – length of overhead line section 1, km, l_{line2} – length of overhead line section 2, km.

The propagation velocity of overhead line section 2 can be also calculated by (7) using only measurements from B side. In both configurations it would be also possible to calculate propagation velocities assuming the availability of measurements from both sides of the line. However, such an approach requires very accurate time synchronization and can lead to additional errors.

$$(7) \qquad v_{line2} = \frac{2l_{line2}}{t_5 - t_4}$$

Fig. 10 depicts the TWs captured during the simulated line closing test. It can be observed that the precise timing of far reflections can be difficult to find. For example, the reflection corresponding to time t_3 seems dispersed and does not have a very prominent peak. At the same time it is virtually impossible to find with certainty the reflection corresponding to time t_5. These uncertainties are reflected in table 5.
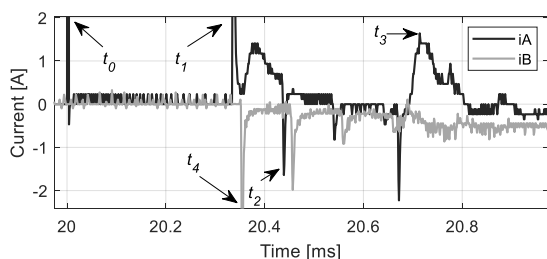

Fig.10. Extracted TWs for line-cable-line configuration

Table 5. Calculation of propagation velocities for line-cable configuration (short cable section case)

Parameter	Value
v_{line1} (5)	298.507 km/ms
v_{cable} (3)	196.078 km/ms
v_{line2} (6)	290.909 km/ms
v_{line2} (7)	t_5 not identified

It can be observed that the propagation velocities calculated based on well-defined TWs (typically not far reflections) are consistent. This applies to the propagation velocities of the first overhead line section and the cable section, values of which are the same as in the previously tested configuration and very close to the expected propagation velocities. However, the calculation of the propagation velocity for the second overhead line section based on the far reflection from the other end of the line is burdened with an error of almost 3% (both overhead line sections are the same). Alternative calculation based on (7) could not be accomplished due to the lack of clear identification of the appropriate TW in the measurements. In case of more complex configurations, it might be necessary to conduct a line closing test on both ends of the line.

Impact on TW-based fault location

In order to investigate the impact of line propagation velocity on the accuracy of TW-based fault location, a series of faults have been simulated on the overhead line section of line-cable configuration in 10% steps starting at 5 km from side A up to 45 km. The expected pattern of first TWs for a fault in the second half of the overhead line section is depicted in fig. 11.
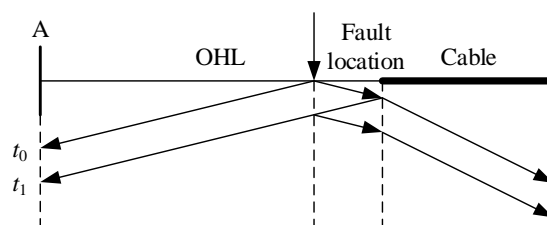

Fig.11. Expected pattern of TW reflections for a fault in overhead section of a line-cable configuration (fault in second half of the line)

First, a single-ended TW-based fault location algorithm is used with the assumption that the faulty half of the line is known. In such a case the absolute location of the fault in the first half of the line can be expressed by (8) and in the second half of the line by (9).

$$(8) \qquad FL = 0.5 v_{line}(t_1 - t_0)$$

$$(9) \qquad FL = l_{line} - 0.5 v_{line}(t_1 - t_0)$$

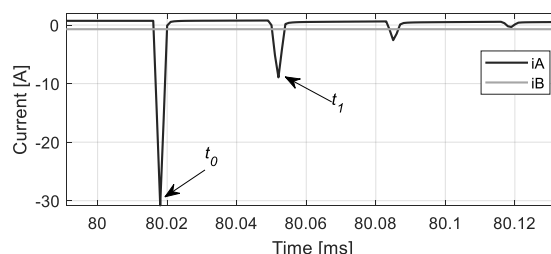An example of TWs captured for a fault located 5 km form the A side is depicted in fig. 12.

Fig.12. Extracted TWs for a fault at 5 km in the overhead line section of a line-cable configuration

The fault location calculation has been done assuming the measured line propagation time of 298.507 km/ms. Two additional variants assuming a 2% and 4% error in the line propagation velocity have been also calculated. The obtained relative errors for each fault location are presented in fig. 13.
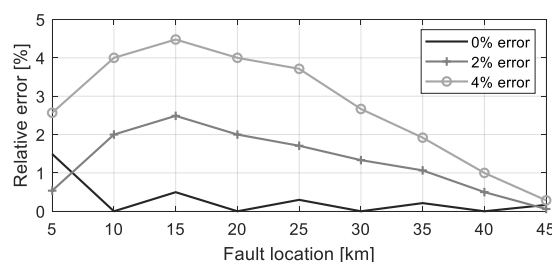

Fig.13. Relative fault location error for single-ended fault location

It can be observed that the maximum error increases linearly, which is expected given (8) and (9). This means that the error in line propagation velocity will directly translate to the error in fault location. This will also affect the identification of a faulty section in certain algorithms, which might be crucial for auto-reclosing blocking schemes in faulty cable section [13].

Next, a double-ended approach is used, in which the timing of the first TWs captured at both line ends, t_0 and t_2. This of course requires synchronization and communication between line ends. Assuming the fault is in the overhead

line section, the fault location can be calculated as follows [2]:

$$(10) \qquad FL = \frac{v_{line}}{2}\left(t_0 - t_2 + \frac{l_{line}}{v_{line}} + \frac{l_{cable}}{v_{cable}}\right)$$

From (10) it can be observed that the fault location accuracy depends on propagation velocity of both sections. The base propagation velocity for the overhead line section is the same as in the previous example and that of the cable section is equal to 196.078 km/ms. Fig. 14 depicts the relative fault location error for cases where an error 2% and 4% was included only in the overhead line propagation velocity, but not in the cable propagation velocity. On the other hand, fig. 15 also depicts the relative fault location errors, but this time errors of 2% and 4% are assumed in propagation velocities of both sections.
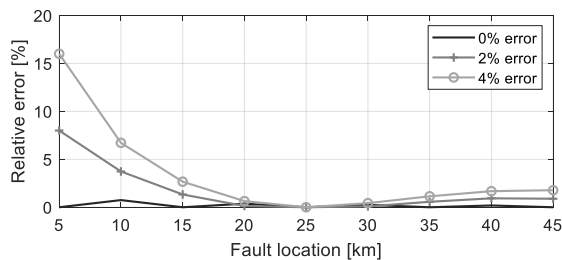

Fig.14. Relative fault location error for double-ended fault location (error only in overhead line propagation velocity)
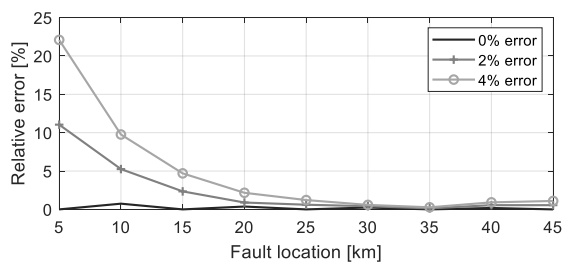

Fig.15. Relative fault location error for double-ended fault location (error in propagation velocities of both sections)

Double-ended fault location has certain advantages over single-ended methods, such as faster fault identification and elimination of the problem of the faulty half of the line identification. However, from figs. 14 and 15 it can be observed that in the case of inaccurate propagation velocity, the fault location error can grow quite high, especially at the beginning of the line. Additionally, since the method relies on the propagation velocities of all sections, the fault location error will increase further (up to over 22%), if propagation velocities of all sections are inaccurate. This will also have an impact on the faulty section identification and would require bigger safety margins for cable sections with auto-reclosing.

Conclusions

The paper presented an analysis of line propagation velocity from a line closing test. The focus of the paper was on hybrid line configurations as they pose a bigger challenge containing both overhead line and cable sections. It has been shown that the propagation velocity of each section can be calculated in different ways (using the timings of different TW reflections). However, it has been observed that it might be difficult to capture the TW information of certain reflections accurately due to the dispersion and attenuation. This is especially true for TWs passing through the cable section. In some cases, it was impossible to identify a TW, which made certain calculations impossible. In case of limited observability of far reflections, it is recommended to perform the line closing test from the other end of the line, which could also serve as validation of results obtained earlier.

The applicability of the calculations has been also tested in a case of a very short cable section (500 m). Assuming a sampling frequency of 1 MHz, it has been shown that the resolution of the measurements may not be sufficient and can result in a considerable error of the propagation velocity. Under such conditions the minimum recommended cable section is 2.5 km. Otherwise, the sampling frequency should be increased to 5 MHz.

Finally, the influence of the propagation velocity error on the fault location accuracy has been investigated. This has been done for a single-ended approach as well as for a double-ended. It could be observed that an error of 4% in the propagation velocity translated to the maximum relative fault location error of over 4% for a single-ended method and over 22% for double-ended method. This proves the importance of accurate propagation velocity calculation.

Authors: dr inż. Paweł Regulski, Politechnika Wrocławska, Wydział Elektryczny, Wybrzeże Wyspiańskiego 27, 50-370 Wrocław, E-mail: pawel.regulski@pwr.edu.pl; prof. dr hab. inż. Waldemar Rebizant, Politechnika Wrocławska, Wydział Elektryczny, Wybrzeże Wyspiańskiego 27, 50-370 Wrocław, E-mail: waldemar.rebizant@pwr.edu.pl; mr. Matthias Kereit, Siemens AG, Berlin, E-mail: matthias.kereit@siemens.com.

REFERENCES

[1] E. O. Schweitzer, III, A. Guzmán, M. V. Mynam, V. Skendzic, and B. Kasztenny, A New Traveling Wave Fault Locating Algorithm for Line Current Differential Relays, *12th International Conference on Developments in Power System Protection*, Copenhagen, Denmark, 2014

[2] S. Marx, Y. Tong, M. V. Mynam, Traveling-Wave Fault Locating for Multiterminal and Hybrid Transmission Lines, *45th Annual Western Protective Relay Conference*, Spokane, Washington, October 16–18, 2018

[3] L. Wang, H. Liu, L. Van Dai, Y. Liu, Novel Method for Identifying Fault Location of Mixed Lines, *Energies*, 2018, Vol. 11, No. 6

[4] R. Zeng, Q. Wu, L. Zhang, Two-terminal traveling wave fault location based on successive variational mode decomposition and frequency-dependent propagation velocity, *Electric Power Systems Research*, Vol. 213, 2022

[5] A. Tabatabaei, M.-R. Mosavi, A. Rahmati, Fault Location Techniques in Power System based on Traveling Wave using Wavelet Analysis and GPS Timing, *Przegląd Elektrotechniczny*, Vol. 88, No. 6, 2012

[6] C. Tao, B. Xing, T. Li, A fault location method for hybrid transmission lines based on empirical Fourier decomposition, *Archives of Electrical Engineering*, Vol. 74, No. 4, 2023

[7] D. López Cortón, J. V. Melado, J. Cruz, R. Kirby, Y. Z. Korkmaz, G. Patti, G. Smelich, Field Experience Using Double-Ended Traveling-Wave Fault Locating Without Relay-to-Relay Communications, *16th International Conference on Developments in Power System Protection*, Newcastle, UK, 2022

[8] Y. Chen, D. Liu, B. Xu, Travelling Wave Single End Fault Location Method based on Network Information, *Przegląd Elektrotechniczny*, Vol. 88, No. 11a, 2012

[9] K. Glik, D. D. Rasolomampionona, R. Kowalik, Detection, classification and fault location in HV lines using travelling waves, *Przegląd Elektrotechniczny*, Vol. 88, No. 1a, 2012

[10] S. Sawai, A. K. Pradhan, Travelling-wave-based protection of transmission line using single-end data, IET Generation, Transmission and Distribution, Vol. 13, No. 20, 2019

[11] D. Rezaei, M. Gholipour, F. Parvaresh, A single-ended traveling-wave-based fault location for a hybrid transmission line using detected arrival times and TW's polarity, Electric Power Systems Research, Vol. 210, 2022

[12] Y. Liu, G. Sheng, Z. He, X. Jiang, A Traveling Wave Fault Location Method for Earth Faults Based on Mode Propagation Time Delays of Multi-measuring Points, Przegląd Elektrotechniczny, Vol. 88, No. 3a, 2012

[13] A. Kulikov, P. Pelevin, A. Loskutov, E. Kryukov, A. Loskutov, Methods for the implementation of automatic reclosing on combined overhead and underground cable power lines 110-500 kV, Przegląd Elektrotechniczny, Vol. 98, No. 7, 2022

[14] I. Daubechies, I. Ten Lectures on Wavelets. CBMS-NSF Regional Conference Series in Applied Mathematics. Philadelphia, PA: Society for Industrial and Applied Mathematics, 1992

[15] W. Rebizant, J. Szafran, A. Wiszniewski, Digital Signal Processing in Power System Protection and Control, Springer, 2011